

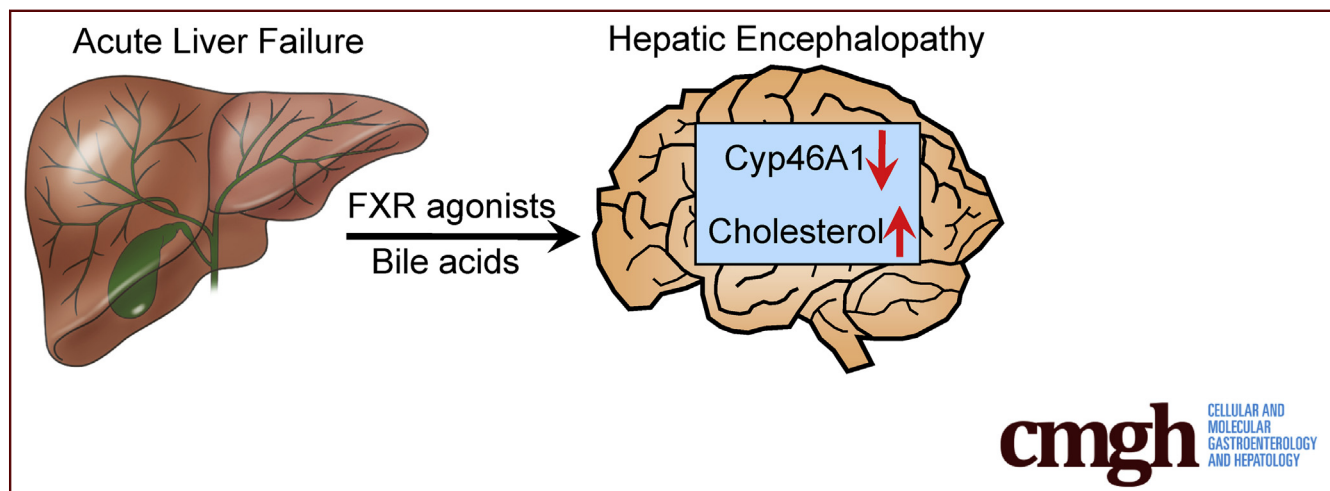
ORIGINAL RESEARCH

FXR-Mediated Cortical Cholesterol Accumulation Contributes to the Pathogenesis of Type A Hepatic Encephalopathy



Matthew McMillin,^{1,2} Stephanie Grant,^{1,2} Gabriel Frampton,^{1,2} Anca D. Petrescu,^{1,2} Jessica Kain,^{1,2} Elaina Williams,^{1,2} Rebecca Haines,² Lauren Canady,² and Sharon DeMorrow^{1,2}

¹Central Texas Veterans Healthcare System, Temple, Texas; ²Department of Medical Physiology, Texas A&M College of Medicine, Temple, Texas



SUMMARY

Concentrations of cholesterol are increased in the brain during acute liver failure–induced hepatic encephalopathy in mice as a result of aberrant farnesoid X receptor–mediated signaling. Strategies aimed at reducing brain cholesterol levels improved neurologic and neuromuscular deficiencies in mice with acute liver failure.

BACKGROUND & AIMS: Hepatic encephalopathy is a serious neurologic complication of acute and chronic liver diseases. We previously showed that aberrant bile acid signaling contributes to the development of hepatic encephalopathy via farnesoid X receptor (FXR)-mediated mechanisms in neurons. In the brain, a novel alternative bile acid synthesis pathway, catalyzed by cytochrome p450 46A1 (Cyp46A1), is the primary mechanism by which the brain regulates cholesterol homeostasis. The aim of this study was to determine if FXR activation in the brain altered cholesterol homeostasis during hepatic encephalopathy.

METHODS: Cyp7A1^{-/-} mice or C57Bl/6 mice pretreated with central infusion of FXR vivo morpholino, 2-hydroxypropyl- β -cyclodextrin, or fed a cholestyramine-supplemented diet were injected with azoxymethane (AOM). Cognitive and

neuromuscular impairment as well as liver damage and expression of Cyp46A1 were assessed using standard techniques. The subsequent cholesterol content in the frontal cortex was measured using commercially available kits and by Filipin III and Nile Red staining.

RESULTS: There was an increase in membrane-bound and intracellular cholesterol in the cortex of mice treated with AOM that was associated with decreased Cyp46A1 expression. Strategies to inhibit FXR signaling prevented the down-regulation of Cyp46A1 and the accumulation of cholesterol. Treatment of mice with 2-hydroxypropyl- β -cyclodextrin attenuated the AOM-induced cholesterol accumulation in the brain and the cognitive and neuromuscular deficits without altering the underlying liver pathology.

CONCLUSIONS: During hepatic encephalopathy, FXR signaling increases brain cholesterol and contributes to neurologic decline. Targeting cholesterol accumulation in the brain may be a possible therapeutic target for the management of hepatic encephalopathy. (*Cell Mol Gastroenterol Hepatol* 2018;6:47–63; <https://doi.org/10.1016/j.jcmgh.2018.02.008>)

Keywords: Cytochrome p450 46A1; Farnesoid X Receptor; Acute Liver Failure; Azoxymethane.

Hepatic encephalopathy is a term used to describe the broad spectrum of neurologic complications that arise from acute (type A hepatic encephalopathy) and chronic (type C hepatic encephalopathy) liver failure. These complications range from mild confusion, learning and memory impairment (which are hallmarks of minimal hepatic encephalopathy), to neuromuscular impairment, asterixis, and ataxia (indications of overt hepatic encephalopathy), and, ultimately, hepatic coma at late stages of disease progression. Cerebral edema, increased intracranial pressure (particularly in acute liver failure), hyperammonemia, and neuroinflammation are associated with hepatic encephalopathy, although the molecular pathogenesis by which hepatic encephalopathy occurs is poorly understood.

A role for aberrant bile acid signaling in the neurologic dysfunction associated with hepatic encephalopathy has been shown in a mouse model of acute liver failure.¹ Specifically, total bile acid content is increased in brain tissue during acute liver failure¹ and these bile acids can be taken up into neurons via the apical sodium bile acid transporter² where they can activate the bile acid nuclear receptor farnesoid X receptor (FXR) and increase the expression of the FXR target gene, small heterodimer partner. Furthermore, strategies to reduce the circulating bile acid concentration by cholestyramine feeding, using mice with genetic deletion of cytochrome p450 7A1 (CYP7A1), or specifically blocking FXR in the brain attenuated the neurologic dysfunction associated with hepatic encephalopathy without altering the underlying liver damage.¹ These data suggest that aberrant bile acid signaling in the brain may play a role in the development of hepatic encephalopathy, although the downstream consequences of this signaling are unknown.

Approximately 25% of the body's cholesterol is found in the brain and its levels are tightly regulated so that fluctuations in dietary cholesterol have minimal effect on brain function.³ In the brain, cholesterol is incorporated into the cell membrane, where it regulates signal transduction pathways, synapse formation, action potentials, and neurotransmitter release.⁴ Furthermore, intracellular cholesterol serves as the precursor for the synthesis of many neurosteroids synthesized in the brain, such as allopregnanolone.⁴ One of the major ways in which the brain clears cholesterol is via its conversion to 24-(S)-hydroxycholesterol, a reaction catalyzed by the enzyme cytochrome p450 46A1 (Cyp46A1).⁵ 24-(S)-hydroxycholesterol then is able to exit the brain and enter the blood stream where it is integrated into the de novo bile acid synthesis pathway in the liver.⁵ Given that bile acids are known to regulate key steps in their biosynthesis pathway, it is conceivable that the aberrant bile acid signaling in the brain may influence the cholesterol clearance pathway. Therefore, this study aimed to assess the cholesterol content in the brain of mice with acute liver failure that may be attributable to bile acid signaling and to determine if strategies to prevent the

buildup of cholesterol in the brain alter the neurologic deficits observed during acute liver failure.

Methods

Materials


All chemicals were purchased from MilliporeSigma (Burlington, MA) unless otherwise noted and were of the highest grade available. The Total Cholesterol and Cholesterol Ester Colorimetric/Fluorometric Assay Kit was purchased from BioVision Inc (Milpitas, CA). Nile Red was purchased from Tokyo Chemical Industry (Tokyo, Japan). The Cyp46A1 antibody was purchased from GeneTex (Irvine, CA). The glyceraldehyde-3-phosphate dehydrogenase (GAPDH) antibody was purchased from GeneTex (Irvine, CA). The primer for Cyp46A1 (catalog no: PPM03965A) and GAPDH (catalog no: PPM02946E) were purchased from Qiagen, SABiosciences (Frederick, MD). FXR vivo-morpholino sequences (FXR morpholino; 5'-CTGAACTGCATCACCATCCTTAGC-3'), FXR mismatch vivo-morpholino sequences (FXR mismatch; 5'-CTCAAAGTGGATCACCATCGTTACC-3'), and Endo-Porter were purchased from Gene Tools (Philomath, OR). Guggulsterone was purchased from Tocris (Minneapolis, MN). Hematoxylin was purchased from Vector Laboratories (Burlingame, CA). Eosin was purchased from MilliporeSigma. Liver enzyme blood chemistry assays were purchased from IDEXX Laboratories, Inc (Westbrook, MA).

Mouse Model of Acute Liver Failure

In vivo experiments were performed using male C57Bl/6 mice (25–30 g; Charles River Laboratories, Wilmington, MA) or Cyp7A1^{-/-} mice bred on a C57Bl/6 background (kind gift from Dr Sandra Erickson, University of California, San Francisco, CA⁶). All animal experiments were approved by the Baylor Scott & White Research Institute Institutional Animal Care and Use Committee and were performed in accordance with the Animal Welfare Act and the Guide for the Care and Use of Laboratory Animals.

Acute liver failure and hepatic encephalopathy were induced using the hepatotoxin azoxymethane (AOM) as previously described.^{1,7–9} Briefly, C57Bl/6 or Cyp7A1^{-/-} mice were injected with AOM (100 mg/kg intraperitoneally) and placed on heating pads set to 37°C to ensure normothermia. To reduce serum and cortical bile acid levels, C57Bl/6 mice were fed a diet supplemented with

Abbreviations used in this paper: AOM, azoxymethane; CYP46A1, cytochrome p450 46A1; CYP7A1, cytochrome p450 7A1; FXR, farnesoid X receptor; GAPDH, glyceraldehyde-3-phosphate dehydrogenase; PBS, phosphate-buffered saline; PFA, paraformaldehyde; RT-PCR, reverse-transcription polymerase chain reaction; 2-H β C, 2-hydroxypropyl- β -cyclodextrin; WT, wild-type.

 Most current article

© 2018 The Authors. Published by Elsevier Inc. on behalf of the AGA Institute. This is an open access article under the CC BY-NC-ND license (<http://creativecommons.org/licenses/by-nc-nd/4.0/>).

2352-345X

<https://doi.org/10.1016/j.jcmgh.2018.02.008>

2% cholestyramine (Dyets, Inc, Bethlehem, PA) or the control diet AIN-93G (Dyets, Inc) for 3 days before the injection of AOM. In parallel, C57Bl/6 mice underwent surgery to implant Alzet brain infusion cannulas coupled to subcutaneous implanted minipumps (Alzet, Cupertino, CA) to directly infuse FXR morpholino or FXR mismatch (1 mg/kg) made up in a 10 μ mol/L Endo-Porter solution to knock down FXR expression in the brain, which effectively knocked down the expression of FXR in neurons located adjacent to the injection site shown and characterized in previous studies.¹ This same approach was used to infuse 2-hydroxypropyl- β -cyclodextrin (2-H β C, 6 mg/kg/day; MilliporeSigma) to inhibit cholesterol accumulation. The infusion cannulas were implanted using the co-ordinates anteroposterior -0.34, mediolateral -1.0, and dorsoventricular -2.0 from Bregma. This surgery was performed 3 days before the injection of AOM to allow the mice to recover before the onset of acute liver failure to minimize mortality.

Starting at 12 hours after injection, mice were monitored at least every 2 hours for body temperature, weight, and neurologic score as previously described.^{7,9} The neurologic score was assessed by an investigator blind to the treatment groups and is a summation of the scores given for the following parameters: pinna reflex, corneal reflex, tail flexion, escape response, righting reflex, and gait. Each parameter was assigned a score between 2 (normal) and 0 (absence of reflexes and presence of severe ataxia), and summed to provide a neurologic score out of 12. At approximately 16 hours after AOM injection, the gait of these experimental mice was examined further using ventral plane imaging technology (DigiGait; Mouse Specifics, Inc, Framingham, MA), which images the underside of animals walking atop a motorized, transparent treadmill belt, thereby generating digital paw prints. These paw prints were analyzed using DigiGait Analysis and Imager software (Mouse Specifics, Inc) and measures of neuromuscular function were quantified, including the paw angle in forelimbs and hind limbs (to measure the degree of external rotation), gait symmetry (ratio of forelimb stepping frequency to hind limb stepping frequency), and the ataxia coefficient for fore and hind limbs (calculated as follows: [maximum stride length - minimum stride length]/average stride length).

Tissue was collected before the onset of neurologic symptoms (preneurologic), when minor ataxia and weakened reflexes were present (minor neurologic), when major ataxia and deficits in reflexes were evident (major neurologic), and at coma, as defined by a loss of righting and corneal reflexes. In experiments involving Cyp7A1^{-/-} mice, cholestyramine-supplemented mice, or 2-H β C-infused mice, only the coma time point was investigated.

Assessment of Liver Damage and Function

Liver damage was assessed by H&E staining according to previously published protocols.⁷ Paraffin-embedded livers were cut into 4- μ m sections and mounted onto positively

charged slides (VWR, Radnor, PA). Slides were deparaffinized and stained with Hematoxylin QS (Vector Laboratories) for 1 minute followed by staining for 1 minute with eosin Y (Amresco, Solon, OH) and rinsed in 95% ethanol. The slides then were dipped into 100% ethanol and subsequently through 2 xylene washes. Coverslips were mounted onto the slides using CytoSeal XYL mounting media (Thermo Fisher Scientific, Waltham, MA). The slides were viewed and imaged using an Olympus BX40 microscope with an Olympus DP25 imaging system (Center Valley, PA).

Liver function was assessed by measuring plasma alanine aminotransferase and aspartate aminotransferase using the IDEXX Catalyst One machine from IDEXX Laboratories, Inc.

In Vitro Primary Neuronal Culture

Primary cortical neurons were isolated and cultured using methodology previously described.⁸ Primary neurons were isolated from postnatal day 1 mouse pups. Mice were decapitated and whole brains were removed. The cortex was isolated and meninges and dura were removed. Cortical tissue was mechanically disrupted and filtered through a 100- μ m filter. Neurons were pelleted by centrifugation at 1400 *g*. Neurons were suspended in media and plated on 12-well plates with 750,000 cells per well. After 24 hours, cells were washed and media was replaced and supplemented with 2% B27 growth supplement. Cells were cultured for 10–12 days and subsequently treated with deoxycholic acid (10 μ mol/L) in the presence or absence of the FXR antagonist guggulsterone (10 μ mol/L) for 24 hours. At this point, cells were lysed and used for immunoblot or reverse-transcription polymerase chain reaction (RT-PCR) analyses.

Assessment of Bile Acid Content in the Brain

The bile acid content of cortex tissue was determined using methodology previously used for other studies.¹ When AOM-treated mice progressed to coma, they were euthanized and transcardially perfused with ice-cold saline to remove the blood from the brain. Cortex homogenates were prepared by calculating the wet weight of brain tissue with subsequent homogenization in 100 mg/mL in ultrapure water using a Miltenyi Biotec gentleMACS Dissociator (San Diego, CA). Homogenates were spun down for 5 minutes at 16,100 *g* and supernatants were collected. Total bile acid content was assessed in homogenates of the frontal cortex following the manufacturer's instructions (IDEXX, Westbrook, ME). Data are reported as the nanomole of bile acid per milligram of cortex tissue protein for each respective analysis.

Measurement of Brain Cholesterol

Total, free, and esterified cholesterol were assessed in brain homogenates using a BioVision Total Cholesterol and Cholesteryl Ester Assay Kit following the manufacturer's instructions with individual samples run in duplicate

and averaged for final values. The subcellular location of cholesterol was assessed using Nile Red staining (for intracellular cholesterol¹⁰) and Filipin III staining (for membrane-bound cholesterol¹¹). Briefly, mice were perfused transcardially with ice-cold phosphate-buffered saline (PBS), followed by 4% paraformaldehyde (PFA) in PBS. Whole brains were rapidly removed and postfixed in PFA overnight at 4°C. Brains were cryoprotected in 30% sucrose (in PBS) and embedded in optimal cutting temperature compound. Thirty-micrometer sections were cut through the frontal cortex region; sections were rinsed in

PBS and further fixed in 4% PFA for 10 minutes at room temperature. Free-floating sections were incubated with Filipin III (0.5 µg/mL in 10% bovine serum albumin/PBS) for 2 hours at room temperature, or with Nile Red (10 µg/mL in PBS) for 30 minutes at room temperature. Sections were washed in PBS, mounted onto microscope slides, and imaged using a Bio-Rad Zoe Fluorescent Cell Imager (Hercules, CA). Field images were quantified for the percentage positive area of Nile Red or Filipin III staining using ImageJ software (National Institutes of Health, Bethesda, MD). Each Nile Red or Filipin III analysis

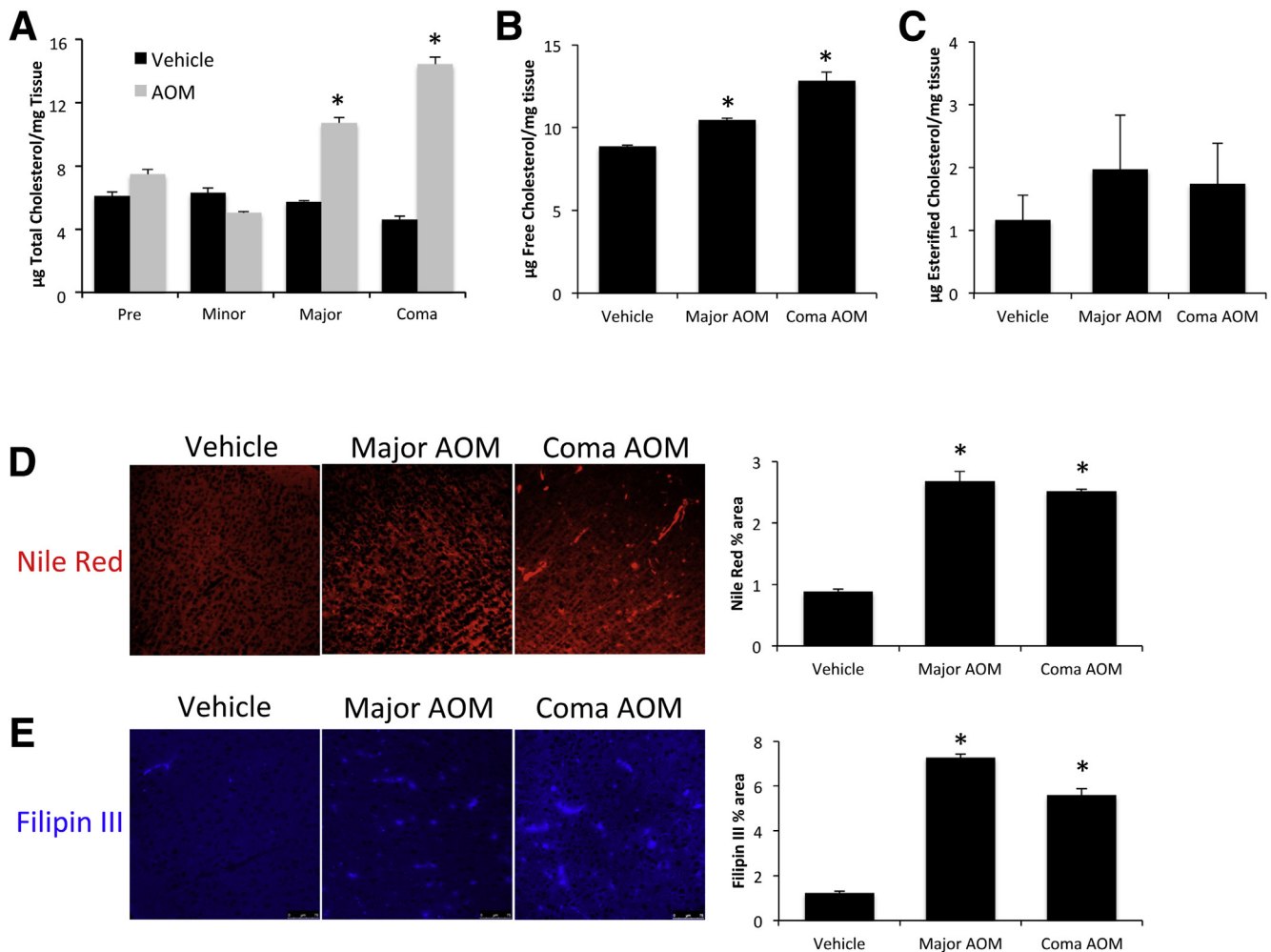


Figure 1. Cholesterol levels are increased in the cortex during AOM-induced hepatic encephalopathy. (A) Total cholesterol levels in the cortex of AOM-treated mice at various stages of neurologic decline including before neurologic decline (Pre), when minor neurologic decline is evident (Minor), when major neurologic decline is evident (Major), and at coma (Coma). Total cholesterol levels are expressed as microgram of cholesterol per milligram of cortex tissue. (B) Free cholesterol levels in the cortex of vehicle and AOM-treated mice at the stages of major neurologic decline and coma. Free cholesterol levels are expressed as microgram of cholesterol per milligram of cortex tissue. (C) Concentration of esterified cholesterol in vehicle and AOM-treated mice at the stages of major neurologic decline and coma. Esterified cholesterol levels are expressed as microgram of esterified cholesterol per milligram of cortex tissue. (D) Nile Red staining and quantification presented as the percentage area in the cortex of vehicle and AOM-treated mice at the major and coma stages of neurologic decline. (E) Filipin III staining and quantification presented as the percentage area in the cortex of vehicle and AOM-treated mice at the major and coma stages of neurologic decline. * $P < .05$ compared with vehicle-treated mice. Data are expressed as means \pm SEM. For all experiments using mouse tissue, $n = 3$ were used per group.

required 10 images taken per brain section with the percentage area quantified as the average of these images per mouse.

Expression of Cyp46A1

RNA was extracted from tissue or primary neurons using an RNeasy Mini Kit (Qiagen, Germantown, MD) according to the manufacturer's instructions. Synthesis of complementary DNA was accomplished using a Bio-Rad iScript Complementary DNA Synthesis Kit. RT-PCR was performed as previously described¹² using commercially available primers designed against mouse Cyp46A1 and GAPDH (SABiosciences). A delta-delta threshold cycle analysis was performed using vehicle-treated tissue or untreated primary

neurons as controls for subsequent experiments.^{13,14} All individual RT-PCR samples were run in duplicates and averaged to determine final values.

Cortex tissue from all treatment groups was homogenized using a Miltenyi Biotec gentleMACS Dissociator and total protein was quantified using a ThermoFisher Pierce BCA Protein Assay kit. Sodium dodecyl sulfate-polyacrylamide gel electrophoresis gels (10% vol/vol) were loaded with 10–20 μ g of protein diluted in Laemmli buffer per each tissue sample. Specific antibodies against Cyp46A1 and β -actin were used. All imaging was performed on an Odyssey 9120 Infrared Imaging System (LI-COR, Lincoln, NE). Data are expressed as the fold change in fluorescent band intensity of target antibody divided by β -actin or GAPDH, which are used as loading controls. The

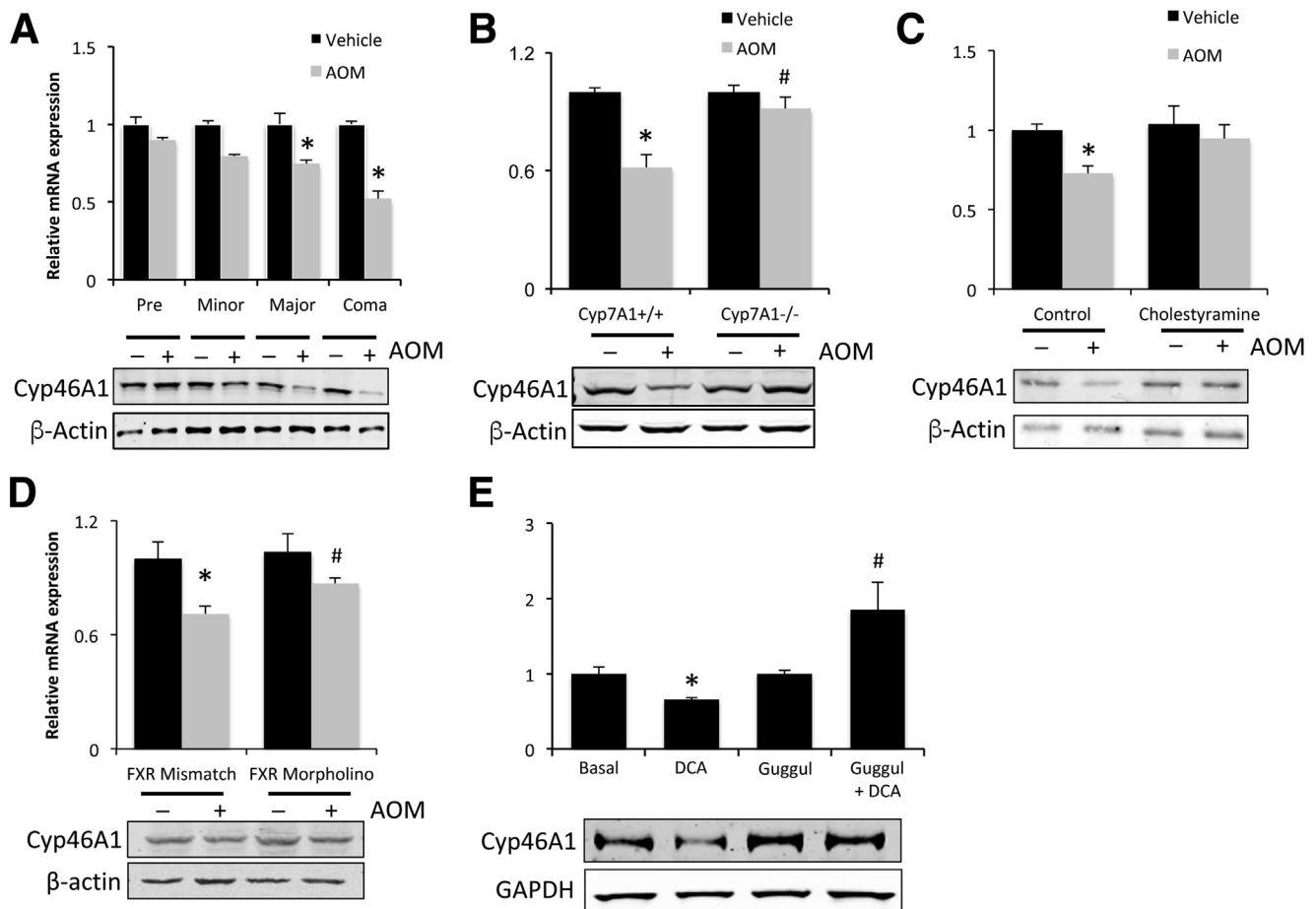


Figure 2. Cortical Cyp46A1 is suppressed in AOM-treated mice via bile acid-dependent FXR signaling. (A) Relative Cyp46A1 mRNA expression (top) and protein expression (bottom) in the cortex of AOM-treated mice at various stages of neurologic decline including before neurologic decline (Pre), when minor neurologic decline is evident (Minor), when major neurologic decline is evident (Major), and at coma (Coma). (B) Relative Cyp46A1 messenger RNA (mRNA) expression (top) and protein expression (bottom) in the cortex of Cyp7A1^{+/+} and Cyp7A1^{-/-} vehicle and AOM-treated mice. (C) Relative Cyp46A1 mRNA expression (top) and protein expression (bottom) in the cortex of control and cholestyramine-fed vehicle and AOM-treated mice. (D) Relative Cyp46A1 mRNA expression (top) and protein expression (bottom) in the cortex of FXR mismatch and FXR morpholino vehicle and AOM-treated mice. (E) Relative Cyp46A1 mRNA expression (top) and protein expression (bottom) in primary mouse neurons treated with 10 μ mol/L deoxycholic acid (DCA) and/or 10 μ mol/L guggulsterone (Guggul). * $P < .05$ compared with vehicle-treated mice of the respective group, # $P < .05$ compared with AOM-treated Cyp7A1^{+/+}, FXR mismatch mice, or DCA-treated primary neurons. Data are expressed as means \pm SEM. For all experiments using mouse tissue or primary neurons, $n = 3$ were used per group.

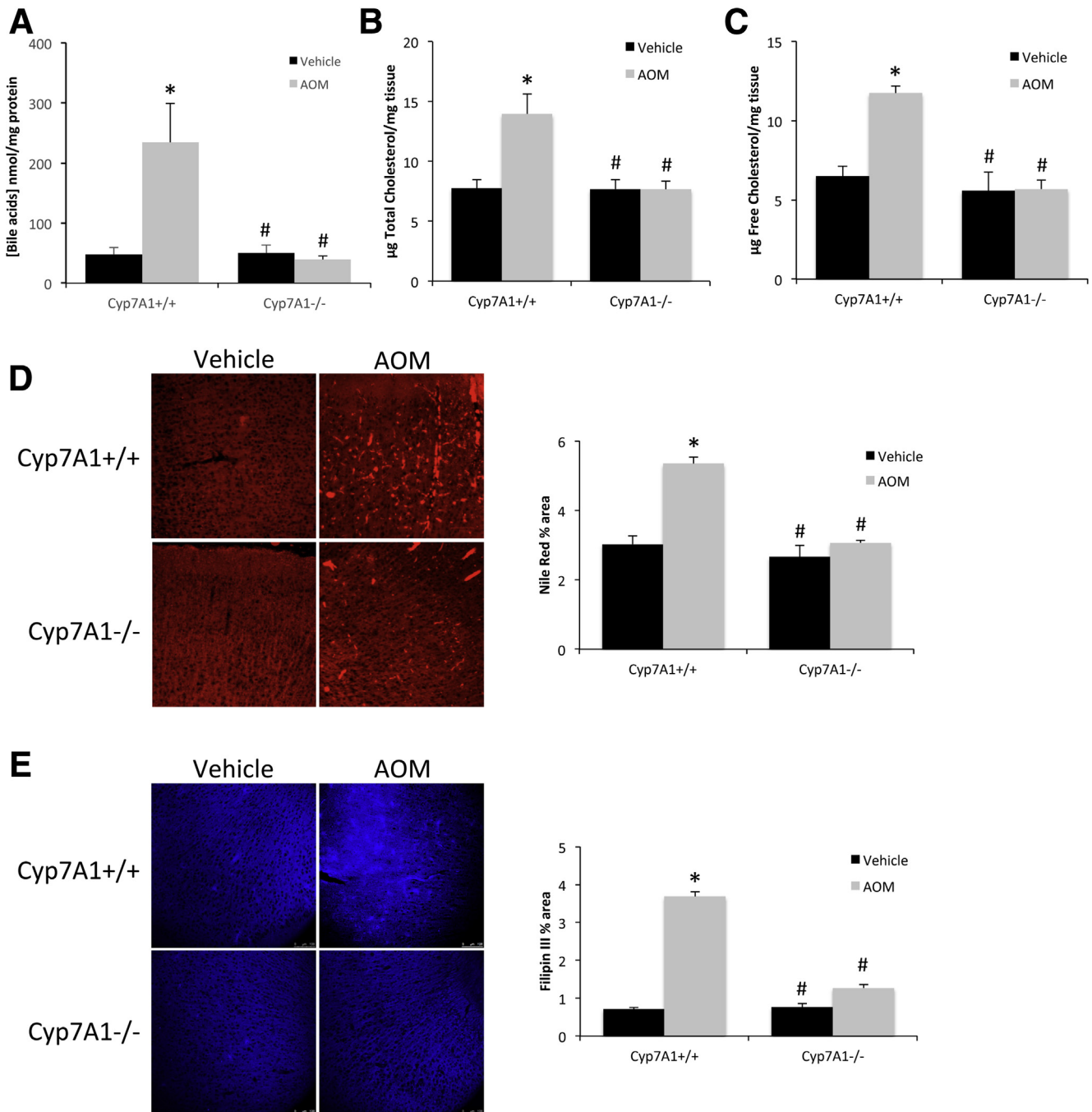


Figure 3. Genetic ablation of Cyp7A1 reduces AOM-induced cholesterol accumulation in the brain. (A) Bile acid concentrations in the cortex of vehicle and AOM-treated Cyp7A1^{+/+} and Cyp7A1^{-/-} mice reported as nanomole of bile acid per milligram of protein. (B) Total cholesterol levels and (C) free cholesterol levels in the cortex of vehicle and AOM-treated Cyp7A1^{+/+} and Cyp7A1^{-/-} mice. Cholesterol levels are expressed as microgram of cholesterol per milligram of cortex tissue. (D) Nile Red staining and quantification were reported as the percentage area in the cortex of vehicle and AOM-treated Cyp7A1^{+/+} and Cyp7A1^{-/-} mice. (E) Filipin III staining and quantification were reported as the percentage area in the cortex of vehicle- and AOM-treated Cyp7A1^{+/+} and Cyp7A1^{-/-} mice. * $P < .05$ compared with vehicle-treated Cyp7A1^{+/+} mice. # $P < .05$ compared with AOM-treated Cyp7A1^{+/+} mice. Data are expressed as means \pm SEM. For all analyses using mouse tissue, $n = 3$ were used per group.

values of vehicle or control groups were used as a baseline and set to a relative protein expression value of 1. Band intensity quantifications were performed using ImageJ software.

Statistics

All statistical analyses were performed using GraphPad Prism software (GraphPad Software, La Jolla, CA). For data that passed normality tests, significance was established

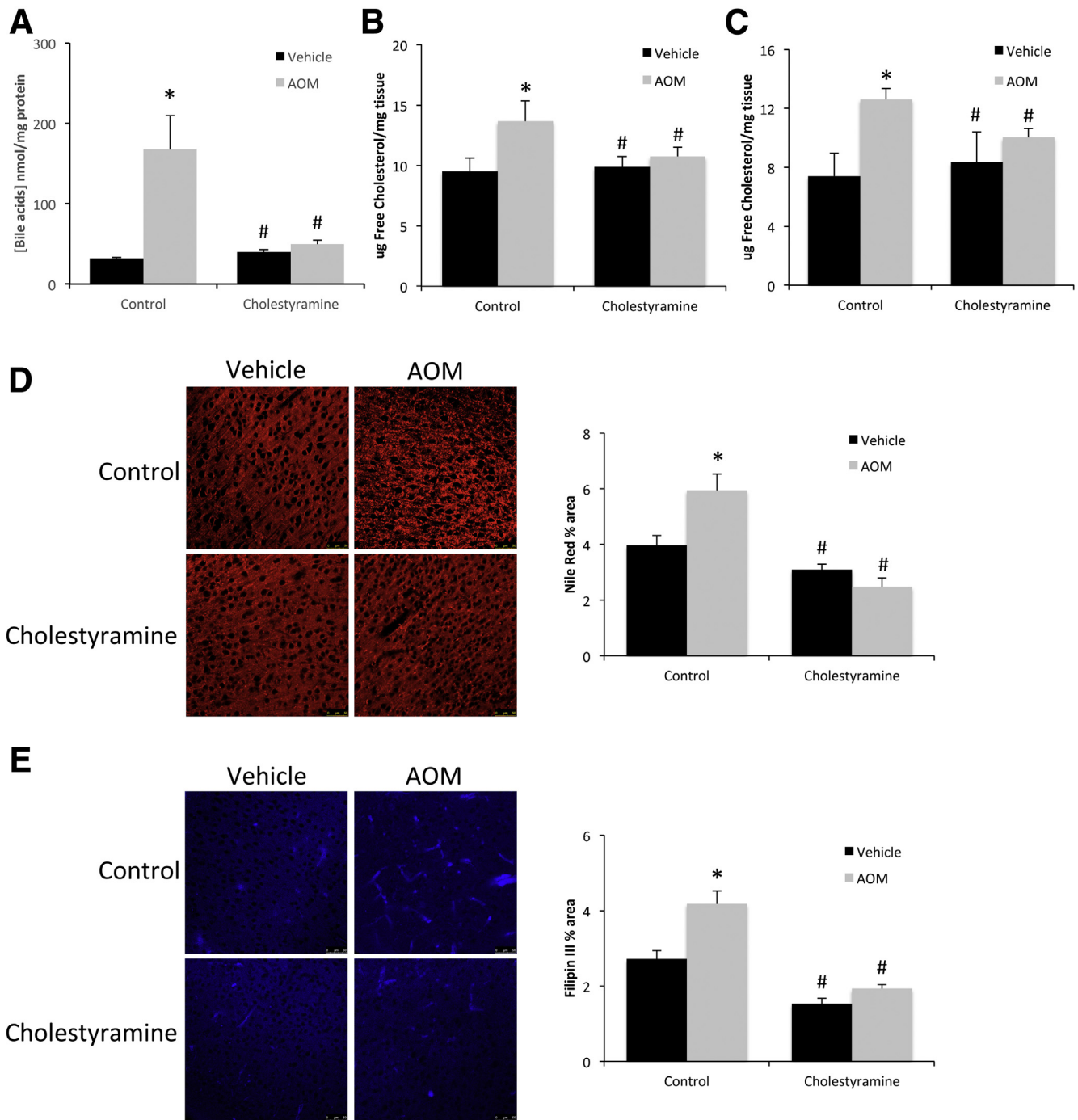
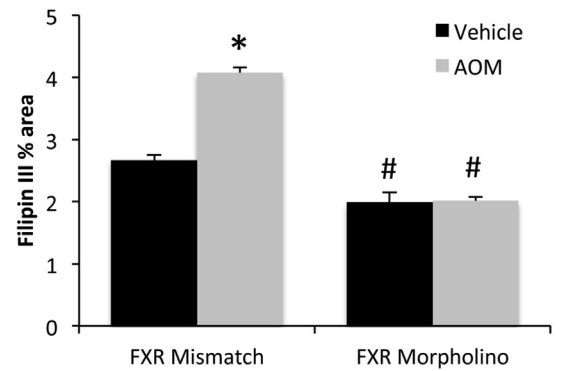
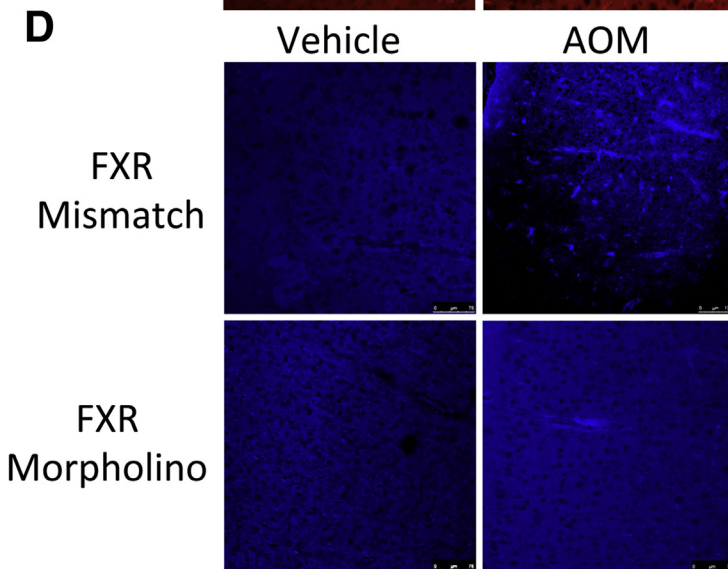
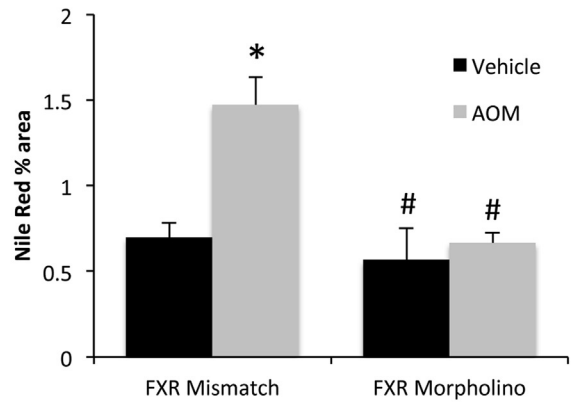
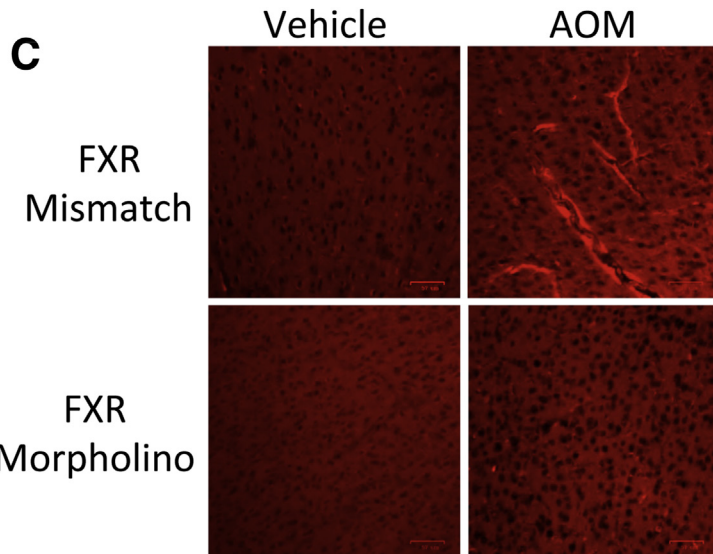
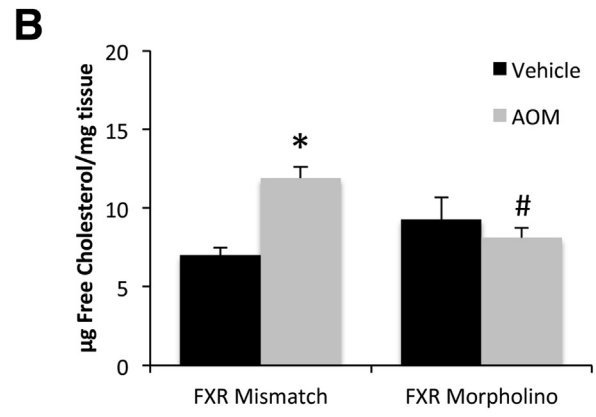
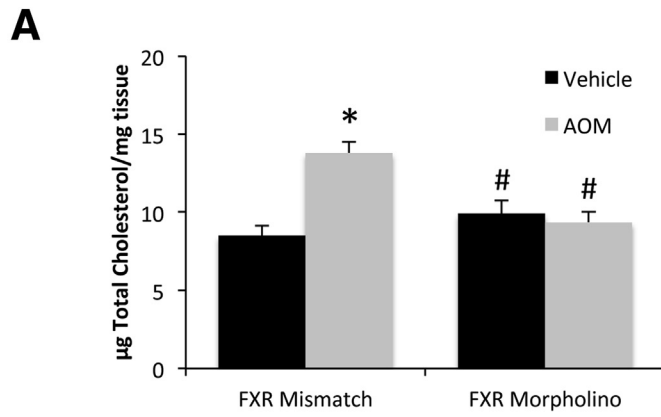


Figure 4. Bile acids induce neural cholesterol accumulation in AOM-treated mice. (A) Bile acid concentrations in the cortex of vehicle and AOM-treated cholestyramine-supplemented mice reported as nanomole of bile acid per milligram of protein. (B) Total cholesterol levels and (C) free cholesterol levels in the cortex of vehicle and AOM-treated cholestyramine-supplemented mice. Cholesterol levels are expressed as microgram of cholesterol per milligram of cortex tissue. (D) Nile Red staining and quantification were reported as the percentage area in the cortex of vehicle and AOM-treated cholestyramine-supplemented mice. (E) Filipin III staining and quantification were reported as the percentage area in the cortex of vehicle and AOM-treated cholestyramine-supplemented mice. * $P < .05$ compared with vehicle-treated control diet fed mice. # $P < .05$ compared with AOM-treated control diet fed mice. Data are expressed as means \pm SEM. For all experiments using mouse tissue, $n = 3$ were used per group.

using the Student's *t* test when differences between 2 groups were analyzed, and analysis of variance when differences between 3 or more groups were compared, followed by the appropriate post hoc test. If tests for normality failed,

2 groups were compared with a Mann-Whitney *U* test or a Kruskal-Wallis ranked analysis when more than 2 groups were analyzed. Results were expressed as means \pm SEM. Differences were considered significant for $P < .05$.



Results

Cortical Cholesterol Concentrations Are Increased in AOM-Treated Mice

We previously showed that aberrant bile acid signaling may contribute to the neurologic complications of acute liver failure.¹ Little is known about the effects of bile acid signaling in the brain. However, the enzymatic machinery for bile acid synthesis has been shown to be present in the brain and is the predominant method by which the brain regulates cholesterol homeostasis.⁵ Therefore, we hypothesized that aberrant bile acid signaling during hepatic encephalopathy might disrupt cholesterol homeostasis in the brain. Indeed, total cholesterol (Figure 1A) and free cholesterol (Figure 1B), but not esterified cholesterol (Figure 1C), were increased significantly with the onset of major neurologic complications in AOM-treated mice. This increase in cholesterol content correlated with increases in both Nile Red (intracellular) and Filipin III (membrane-bound) staining in the brain (Figure 1D and E). Taken together, these data indicate that the total cholesterol content is increased in the brain during acute liver failure, which is distributed both intracellularly and in the membrane.

AOM-Treated Mice Have Reduced Cortical Cyp46A1 Activity

To determine if the cholesterol buildup may be owing to an impaired clearance pathway, the expression of Cyp46A1 was assessed in mice with acute liver failure. Expression of Cyp46A1 messenger RNA and protein was down-regulated in the cortex of AOM-treated mice showing neurologic symptoms of hepatic encephalopathy (Figure 2A), suggesting that the buildup in cholesterol in the brain might be attributable to an impaired clearance pathway. Interestingly, this down-regulation of Cyp46A1 was not evident in mouse models showing attenuated AOM-induced aberrant bile acid signaling in the brain.¹ Specifically, we previously have shown that increases in serum and cortical bile acid content are not evident in Cyp7A1^{-/-} mice after AOM injection, which correlated with a delay in the neurologic decline associated with acute liver failure.¹ Furthermore, we previously have shown that the effects of bile acid signaling in the development of hepatic encephalopathy are attributable, in part, to FXR signaling in neurons and specific knockdown of FXR activity in the brain using a cholestyramine-supplemented diet or direct infusion of FXR morpholino delayed the neurologic decline associated with AOM-induced acute

liver failure.¹ In Cyp7A1^{-/-} mice, cholestyramine-fed mice, or mice infused with FXR morpholino, the down-regulation of Cyp46A1 expression in response to AOM injection was attenuated (Figure 2B–D). To determine if the suppression of Cyp46A1 was attributable to a direct action of FXR-mediated signaling and not a reflection of the degree of neurologic impairment in these mice, primary neurons were treated with deoxycholic acid, a known agonist of FXR,¹⁵ which decreased the expression of Cyp46A1. This could be prevented by pretreatment with the FXR antagonist guggulsterone (Figure 2E).

Reducing Cortical Bile Acid Levels Alleviates Cholesterol Accumulation in AOM-Treated Mice

The pathway mediated by Cyp46A1 is a primary method regulating cholesterol homeostasis in the brain.⁵ Therefore, we assessed whether preventing the suppression of Cyp46A1 expression in mouse models in which aberrant cortical bile acid signaling was attenuated could influence the degree of cholesterol buildup. Initially, Cyp7A1^{-/-} mice were assessed during AOM-induced hepatic encephalopathy for their relative increase of cortical bile acids compared with Cyp7A1^{+/+} (wild-type [WT]) mice. Concentrations of cortical bile acids were increased significantly in WT AOM-treated mice and this effect was absent in Cyp7A1^{-/-} mice (Figure 3A). A similar trend was seen regarding cholesterol because an increase in total and free cholesterol content was observed in the WT mice after AOM injection that was not evident in Cyp7A1^{-/-} mice (Figure 3B and C). Furthermore, the increase in intracellular cholesterol (Nile Red staining) (Figure 3D) and membrane-bound cholesterol (Filipin III staining) (Figure 3E) observed in WT mice after AOM injection was absent in Cyp7A1^{-/-} mice.

To better validate that the effects observed in Cyp7A1^{-/-} mice were caused by bile acids alone and not a congenital or strain-specific effect, C57Bl/6 mice were fed a diet supplemented with 2% cholestyramine to reduce bile acid levels. Cholestyramine supplementation was found to significantly reduce the concentration of cortical bile acids in AOM-treated mice compared with the AOM-treated control diet-fed mice (Figure 4A). This effect correlated with a reduction in total and free cholesterol levels in the AOM-treated, cholestyramine-supplemented mice compared with AOM-treated controls (Figure 4B and C). In addition, the increase in Nile Red (Figure 4D) and Filipin III staining (Figure 4E) observed after AOM treatment was reduced by cholestyramine pretreatment, showing a reduction of intracellular and free cholesterol, respectively, after cholestyramine supplementation.

Figure 5. (See previous page). **FXR exacerbates neural cholesterol accumulation in AOM-treated mice.** (A) Total cholesterol levels and (B) free cholesterol levels in the cortex of vehicle and AOM-treated FXR mismatch and FXR morpholino-infused mice. Cholesterol levels are expressed as microgram of cholesterol per milligram of cortex tissue. (C) Nile Red staining and quantification were reported as the percentage area in the cortex of vehicle and AOM-treated FXR mismatch and FXR morpholino-infused mice. (D) Filipin III staining and quantification were reported as the percentage area in the cortex of vehicle and AOM-treated FXR mismatch and FXR morpholino-infused mice. **P* < .05 compared with vehicle-treated FXR mismatch-infused mice. #*P* < .05 compared with AOM-treated FXR mismatch-infused mice. Data are expressed as means ± SEM. For all experiments using mouse tissue, *n* = 3 were used per group.

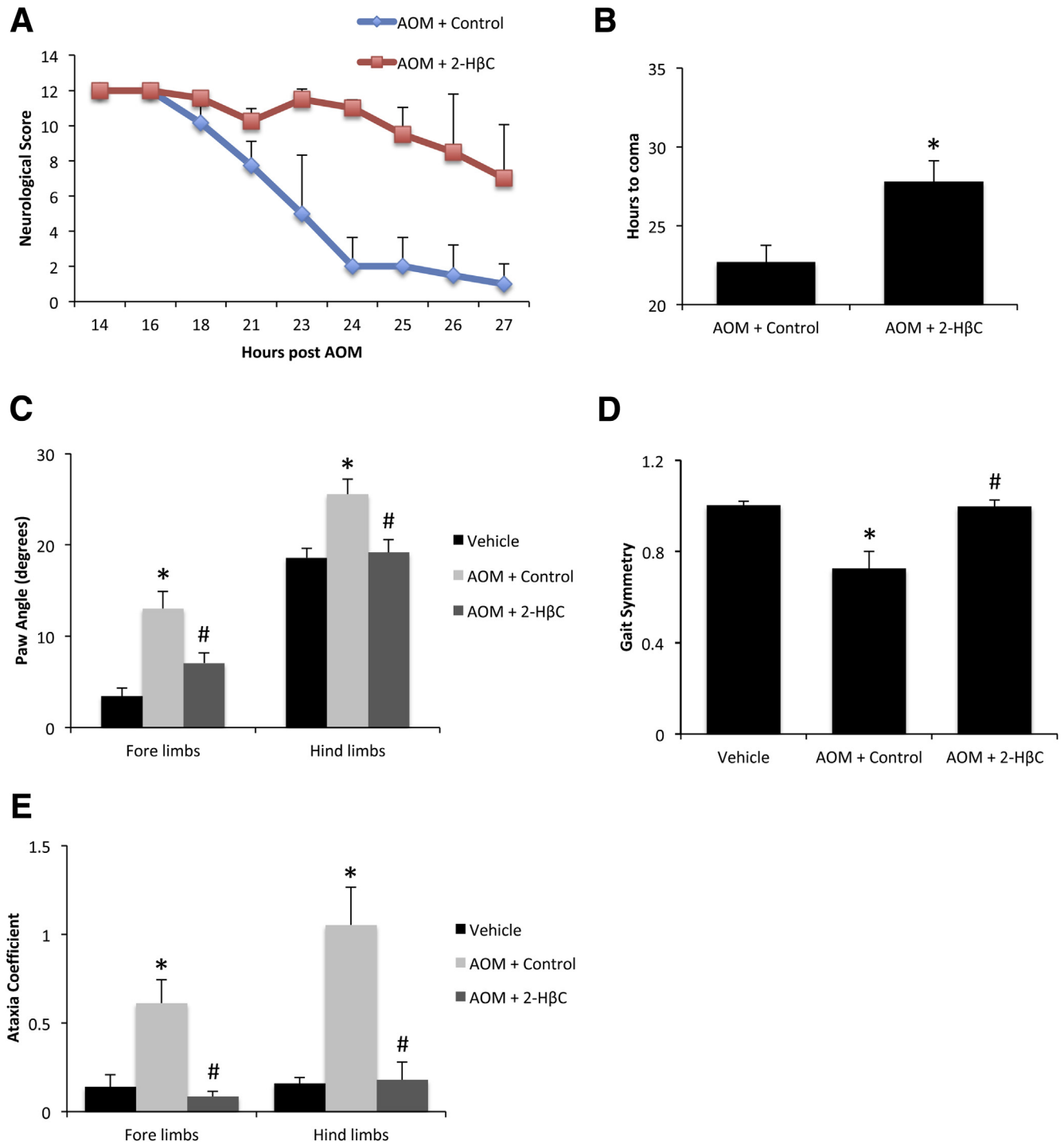


Figure 6. Intracerebroventricular infusion of 2-H β C reduces neurologic decline in AOM-treated mice. (A) Neurologic score in AOM-treated mice infused with control or 2-H β C. A neurologic score of 12 indicates normal function, with the score decreasing as neurologic impairment occurs. (B) Time in hours for AOM-treated control and 2-H β C-infused mice to progress to hepatic coma. (C) Paw angle in degrees of the forelimbs and hind limbs of AOM-treated control and 2-H β C-infused mice. (D) Gait symmetry of vehicle, AOM-treated control, and AOM-treated 2-H β C-infused mice. (E) Ataxia coefficient of the forelimbs and hind limbs of vehicle, AOM-treated control, and AOM-treated 2-H β C-infused mice. * $P < .05$ compared with vehicle-treated mice or AOM + control mice for the time-to-coma analysis. # $P < .05$ compared with AOM-treated control-infused mice. Data are expressed as means \pm SEM. For all experiments assessing behavior and neurologic function, $n = 6$ were used for AOM-treated groups and $n = 4$ for vehicle-treated groups.

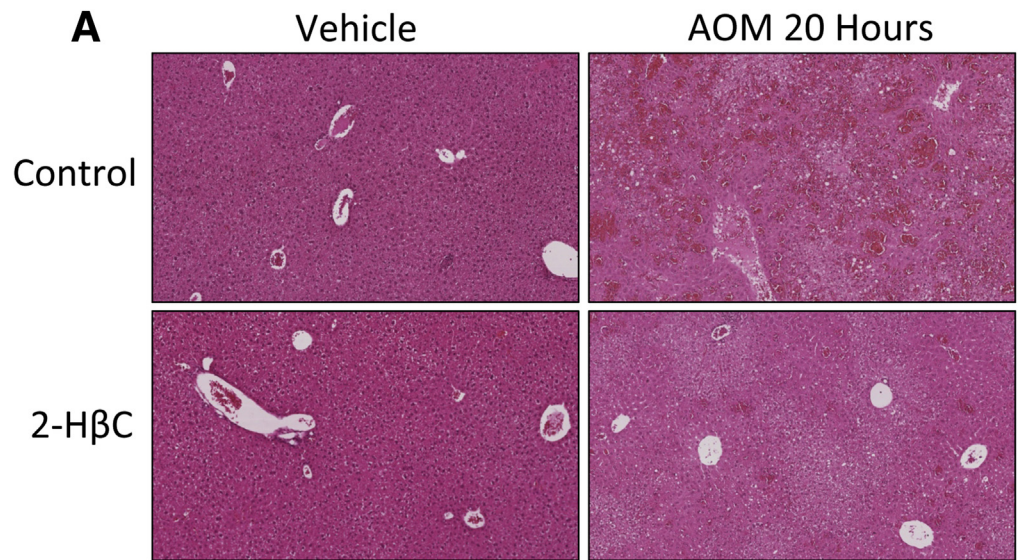
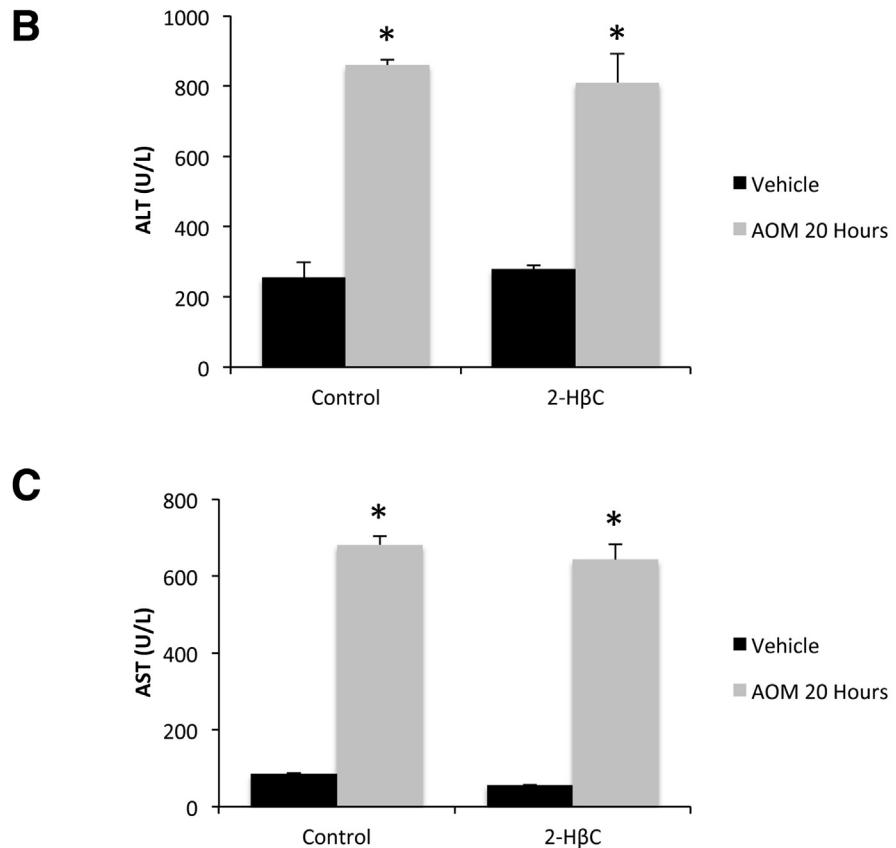


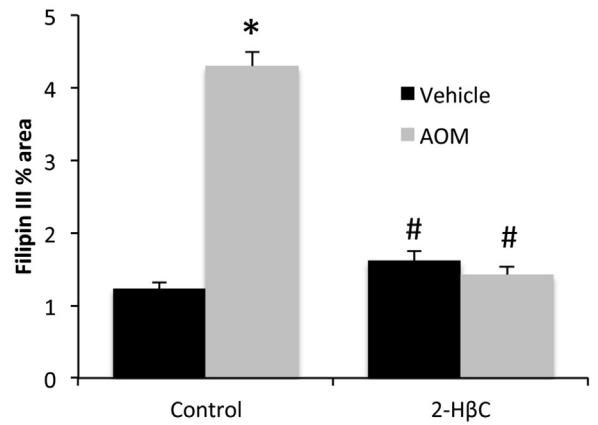
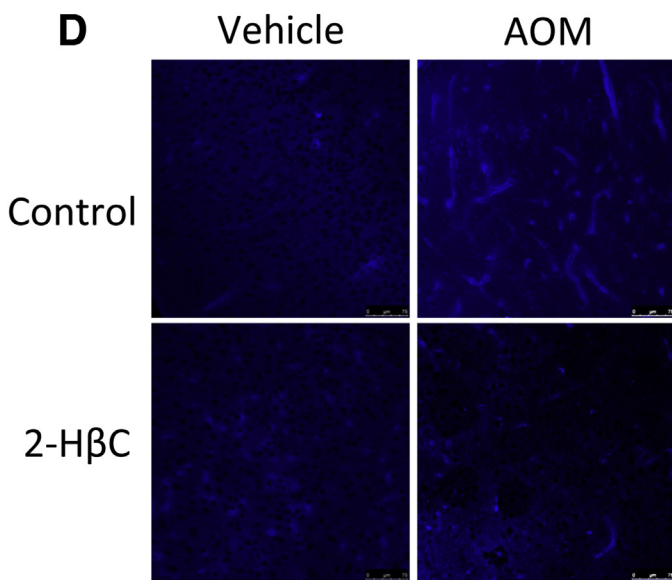
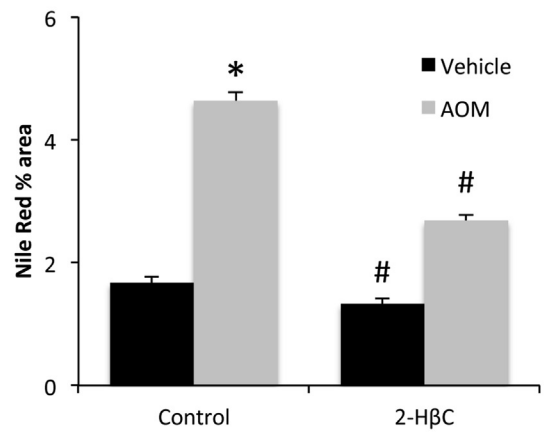
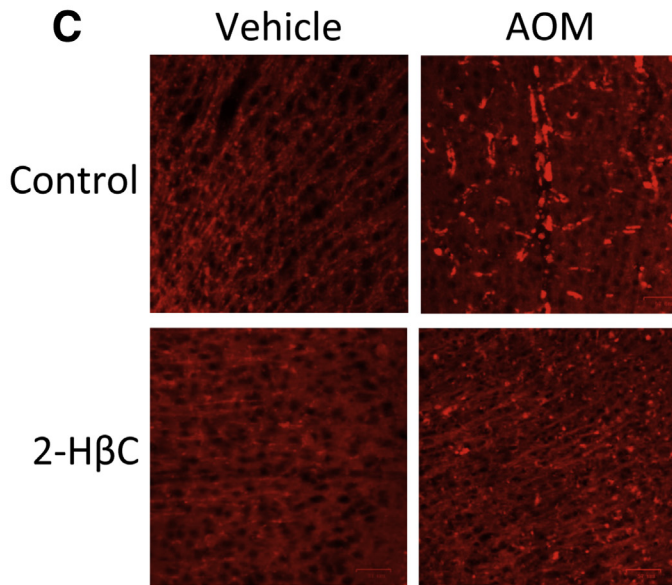
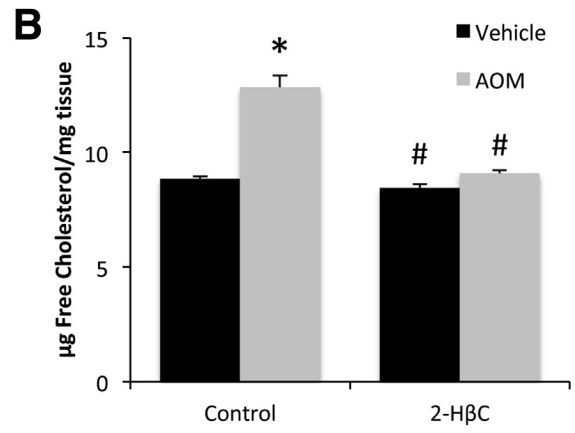
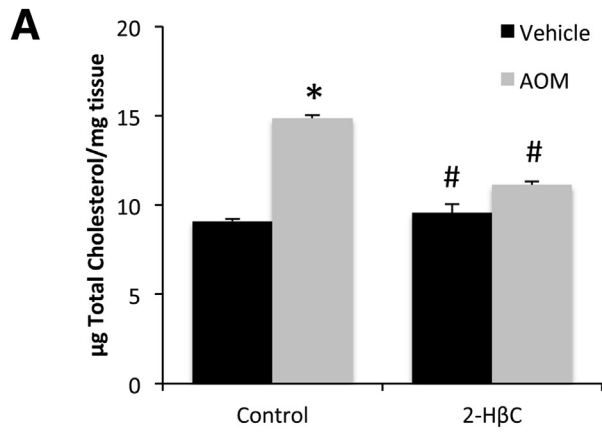
Figure 7. Intracerebroventricular infusion of 2-HβC does not influence liver function. (A) H&E staining of liver sections from vehicle and 20-hour post-AOM injection mice that were infused with control or 2-HβC. (B) Alanine aminotransferase (ALT) and (C) aspartate aminotransferase (AST) concentrations in the plasma of vehicle and 20-hour post-AOM injection mice that were infused with control or 2-HβC. * $P < .05$ compared with vehicle-treated control-infused mice. Data are expressed as means \pm SEM. For ALT and AST measurements, $n = 4$ were used for AOM-treated groups and $n = 3$ for vehicle-treated groups.



FXR Signaling Promotes Cholesterol Accumulation in the Cortex

If bile acids are the primary contributor to the accumulation of cortical cholesterol observed in AOM-treated mice, then this effect could be a result of bile acid-receptor-mediated signaling. Although bile acids can signal through both G-protein-coupled receptors and nuclear receptors,

we previously have shown that FXR is present in neurons and FXR signaling contributes to neurologic decline in AOM-treated mice.¹ Therefore, the approach taken was to reduce neuronal FXR protein expression through FXR morpholino infusion in vehicle and AOM-treated mice and assess cholesterol concentrations. Similar to what was observed in *Cyp7A1*^{-/-} and cholestyramine-supplemented



mice, total and free cholesterol (Figure 5A and B), as well as intracellular (Figure 5C) and membrane-bound (Figure 5D) cholesterol, were increased in AOM-treated mice infused with a control mismatched vivo morpholino sequence and this effect was attenuated in mice infused with FXR morpholino.

Infusion of 2-H β C Reduces Neurologic Deficits and Cortical Cholesterol Levels in AOM-Treated Mice

To determine whether cholesterol buildup in the brain plays a role in the neurologic deficits associated with acute liver failure, mice were infused with 2-H β C into the lateral ventricle. Treatment of mice with 2-H β C before AOM injection significantly delayed the neurologic decline (Figure 6A) and increased the time taken to reach hepatic coma (Figure 6B). Besides these neurologic measures, neuromuscular complications during hepatic encephalopathy also were assessed. Specifically, control mice walked with a paw angle of approximately 3.5° (forelimb) or 18° (hind limb) of external rotation, which is consistent with previously published studies¹⁶ (Figure 6C). In AOM-treated mice, there was an increased degree of external rotation of both the forelimbs and hind limbs, indicating a splaying of the paws often seen during ataxia.¹⁶ Treatment with 2-H β C reduced the paw angle of AOM-treated mice to values similar to controls (Figure 6C). Second, gait symmetry, defined as the ratio of forelimb stepping frequency to hind limb stepping frequency was effectively 1 in control mice as expected, but this was reduced significantly in mice injected with AOM (Figure 6D), indicating the mice were stepping more frequently on the hind limbs than forelimbs to compensate for the neuromuscular deficits in the hind limbs. Infusion with 2-H β C before AOM injection returned the gait symmetry to control levels (Figure 6D). Finally, we measured the ataxia co-efficient, which is an index of step-to-step variability for each limb. Control mice had a low ataxia co-efficient in both the forelimbs and hind limbs (Figure 6E), indicating a relatively consistent stride length in all limbs. However, mice with AOM-induced acute liver failure had a significantly higher ataxia co-efficient, indicating a greater variability in stride length, and infusion of 2-H β C returned the ataxia co-efficient back to control levels (Figure 6E).

The central infusion of 2-H β C was chosen over systemic administration to allow for the delineation of direct neuroprotective effects of 2-H β C on the development of hepatic encephalopathy vs the potential indirect hepatoprotective effects that then would impact the subsequent neurologic complications. Confirmatory experiments were performed

to ensure that the local central infusion of 2-H β C had no effect on the underlying AOM-induced liver damage. The degree of liver damage significantly increased after AOM injection as shown by H&E staining (Figure 7A), serum alanine aminotransferase (Figure 7B), and aspartate aminotransferase (Figure 7C) to a similar degree as shown previously,^{1,7-9} and these results were similar to mice infused with 2-H β C before AOM injection (Figure 7). These data indicate that central infusion of 2-H β C does not have any hepatoprotective effects against AOM-induced hepatotoxicity and that the protective effects of 2-H β C observed on the development of hepatic encephalopathy result from the direct actions in the brain.

Finally, 2-H β C treatment has been shown previously to prevent excessive cholesterol buildup in the brain in models of Niemann–Pick type C disease without depleting it completely.¹⁷ Similarly, 2-H β C infusion into the brain did not decrease the basal levels of cholesterol but did prevent the AOM-induced buildup in total (Figure 8A) and free (Figure 8B) cholesterol content in the cortex. Furthermore, 2-H β C treatment attenuated the AOM-induced increase in Nile Red (Figure 8C) and Filipin III (Figure 8D) staining. Taken together, these data suggest that neuroprotective actions of 2-H β C likely are owing to the prevention of cholesterol buildup in the brain and that the increase in cortical cholesterol observed after AOM likely is contributing to the neurologic complications of acute liver failure.

Discussion

The major findings of this study pertain to the potential downstream consequences of aberrant bile acid signaling in the brain during acute liver failure and its subsequent role in the development of hepatic encephalopathy. The data presented here show that, similar to the liver, FXR signaling in the brain can alter cholesterol homeostasis by regulating Cyp46A1-mediated cholesterol clearance pathways, leading to a buildup up of cholesterol in the brain during acute liver failure. Furthermore, a treatment regimen designed to prevent the accumulation of cholesterol had protective effects against the cognitive and neuromuscular dysfunction associated with hepatic encephalopathy. Taken together, our data suggest that a downstream consequence of FXR signaling in the brain may be the accumulation of cholesterol, which has implications on the pathogenesis of hepatic encephalopathy.

For this study, we used the AOM model of acute liver injury. This model was chosen for the following reasons: (1) it is the only model in mice for acute liver failure leading to the development of hepatic encephalopathy recommended

Figure 8. (See previous page). Cortex cholesterol accumulation in AOM-treated mice is reduced by 2-H β C infusion. (A) Total cholesterol levels and (B) free cholesterol levels in the cortex of vehicle and AOM-treated control and 2-H β C-infused mice. Cholesterol levels are expressed as microgram of cholesterol per milligram of cortex tissue. (C) Nile Red staining and quantification were reported as the percentage area in the cortex of vehicle and AOM-treated control and 2-H β C-infused mice. (D) Filipin III staining and quantification were reported as the percentage area in the cortex of vehicle and AOM-treated control and 2-H β C-infused mice. * $P < .05$ compared with vehicle-treated control-infused mice. # $P < .05$ compared with AOM-treated control-infused mice. Data are expressed as means \pm SEM. For all experiments using mouse tissue, $n = 3$ were used for all groups.

by a subcommittee of the International Society of Hepatic Encephalopathy and Nitrogen Metabolism¹⁸; (2) unlike other mouse models, the AOM model of hepatic encephalopathy is reproducible, reversible to a certain degree, has a reasonable therapeutic window, and produces neurologic decline ultimately resulting in liver-related death (similar to that observed in human beings) as long as the body temperature and other physiological parameters are tightly controlled¹⁹; and (3) use of other common clinically relevant drugs involved in drug-induced liver failure, such as acetaminophen, do not cause hepatic encephalopathy in mice. Recently, it was suggested that AOM is a flawed model of hepatic encephalopathy because AOM may be directly toxic to brain endothelial cells, thereby opening the blood-brain barrier.²⁰ However, we recently showed that direct treatment of endothelial cells with AOM *in vitro* does not lead to increased monolayer permeability when these cells were co-cultured with primary astrocytes.²¹ In addition, increased permeability of the blood-brain barrier after AOM *in vivo* occurs at the later stages of encephalopathy well beyond the onset of neurologic symptoms^{21,22} and is dependent on a certain degree of systemic inflammation.²³ Together, these *in vivo* reports do not support the idea that AOM is directly causing leakiness of the blood-brain barrier, but rather is a consequence of liver failure and the resulting complications that arise.

Our current understanding of the pathogenesis of hepatic encephalopathy largely has centered around the buildup of serum and cortical ammonia during acute liver failure, which can act synergistically with peripheral and central inflammation to precipitate the neurologic difficulties observed during hepatic encephalopathy.^{24,25} However, the increase of circulating bile acids observed after liver damage has been identified as another possible culprit contributing to the complex etiology of hepatic encephalopathy.^{1,7,26–28} We previously showed that aberrant bile acid signaling in neurons, either through FXR or sphingosine-1 phosphate receptor 2, contributes to the neurologic deficits and neuroinflammatory processes observed during acute liver failure.^{1,7} Interestingly, bile acid signaling recently was implicated in a number of other neurologic disorders,²⁹ although a common consequence of bile acid signaling in the brain during these neurologic disorders is not clear.

The current study aimed to elucidate the downstream consequences of FXR-mediated signaling and its consequences on cortical cholesterol accumulation. The cortex was the primary brain region investigated because it is functionally impaired during hepatic encephalopathy and previous research has shown that FXR, apical sodium-dependent bile acid transporter, and small heterodimer partner are expressed in cortical neurons and these neurons can transport cholyl-lysyl-fluorescein, a fluorescent bile acid-like substrate, across the cell membrane.^{1,30,31} In this study, we showed that expression of the enzyme Cyp46A1 was down-regulated in the cortex during acute liver failure and that strategies to reduce cortical bile acid levels or FXR signaling prevented this down-regulation. Cyp46A1 is a brain-specific cytochrome p450 that regulates cholesterol

homeostasis by oxidizing cholesterol to 24-(S)-hydroxycholesterol, which can be removed more readily from the brain.⁵ The data presented here show a regulatory effect of both bile acids and FXR-mediated signaling on the expression of Cyp46A1, although the precise mechanism is unknown. It is possible that other FXR ligands or other bile acid receptors influence Cyp46A1 expression and cholesterol accumulation and these topics warrant further investigation. Recent studies have shown that the promoter region of Cyp46A1 is regulated by the transcription factor SP-1.³² Given that a functional interaction has been shown between FXR and SP-1 in the regulation of other genes involved in lipid metabolism,³³ it is conceivable that bile acids could exert their effects on Cyp46A1 expression via the interaction between FXR and SP-1.

Imbalances in cholesterol homeostasis in the brain have been implicated in a number of neurologic disorders.^{3,34} Some disorders, such as Smith-Lemli Opitz Syndrome³⁵ and Huntington's Disease,³⁶ are associated with a reduction in brain cholesterol, whereas others, such as Niemann-Pick type C disorder, feature an accumulation in cholesterol.³⁷ Consistent with these reports, our data suggest that cholesterol accumulation also may be a component of the pathophysiological processes associated with hepatic encephalopathy. Cholesterol has many functions in the physiological function of the brain. For example, cholesterol is a precursor for the synthesis of neurosteroids such as allopregnanolone and tetrahydrodeoxycorticosterone. Cholesterol is transported into the mitochondria through a translocator protein, where the biosynthesis of these neurosteroids occurs. The expression and binding activity of the translocator protein, as well as neurosteroid synthesis, are up-regulated in human and rodent models of hepatic encephalopathy.³⁸ Our data suggest that it may be the consequences of aberrant bile acid signaling in the brain leading to an increase in cholesterol that supplies the substrate needed for the increased production of neurosteroids. Second, cholesterol is a major component of the cell membrane and can influence the activity of receptors and other signaling molecules.³⁹ In neurons in particular, the cholesterol content in the membrane can alter neurotransmitter release and the rate of firing of action potentials,^{40–42} and agents that deplete cholesterol from the presynaptic membrane increase the frequency of spontaneous neurotransmitter release.⁴⁰ Given that the release and activity of a number of neurotransmitter systems are dysregulated in hepatic encephalopathy, it also is conceivable that bile acid-mediated dysregulation of cholesterol homeostasis may be altering neurotransmitter release. The data presented here indicate that both intracellular and membrane-bound cholesterol are altered in our mouse model of hepatic encephalopathy. Therefore, it is likely that our data has implications in both the enhanced neurosteroid synthesis and altered neurotransmitter function observed in hepatic encephalopathy and further studies are warranted.

In this study, we used a constant central infusion of the cholesterol sequestrant 2-H β C to prevent the buildup of cholesterol in the brain. This, and related cyclodextrins, have been proposed as a safe and effective treatment for the

management of Niemann–Pick type C disease.^{43–45} Indeed, intrathecal, intracerebroventricular, or intravenous administration of cyclodextrins have had proven therapeutic value to varying degrees in clinical trials.^{43,44} As stated earlier, we implanted the cannulas before the onset of liver damage and administered 2-H β C directly into the brain to differentiate the direct neuroprotective effects of 2-H β C on hepatic encephalopathy vs the potential indirect protective effects on the liver, which is important to delineate from a mechanistic standpoint. However, further studies are needed to determine the therapeutic potential of 2-H β C for the management of hepatic encephalopathy involving a more feasible route of administration given after the onset of acute liver failure.

In conclusion, the data presented here show that one potential downstream consequence of aberrant FXR signaling in the brain during hepatic encephalopathy is the accumulation of intracellular and membrane-associated cholesterol. Furthermore, we have shown that strategies preventing the accumulation of cholesterol proved neuroprotective against the neurologic complications of acute liver failure. Taken together, our data suggest that cholesterol may play a novel role in the pathogenesis of hepatic encephalopathy and may prove to be a viable target for the development of novel adjunct therapies for the management of hepatic encephalopathy.

References

- McMillin M, Frampton G, Quinn M, Ashfaq S, de los Santos M 3rd, Grant S, DeMorrow S. Bile acid signaling is involved in the neurological decline in a murine model of acute liver failure. *Am J Pathol* 2016;186:312–323.
- McMillin M, Frampton G, Quinn M, Divan A, Grant S, Patel N, Newell-Rogers K, DeMorrow S. Suppression of the HPA axis during cholestasis can be attributed to hypothalamic bile acid signaling. *Mol Endocrinol* 2015;29:1720–1730.
- Orth M, Bellosta S. Cholesterol: its regulation and role in central nervous system disorders. *Cholesterol* 2012;2012:292598.
- Cartocci V, Servadio M, Trezza V, Pallottini V. Can cholesterol metabolism modulation affect brain function and behavior? *J Cell Physiol* 2017;232:281–286.
- Lund EG, Xie C, Kotti T, Turley SD, Dietschy JM, Russell DW. Knockout of the cholesterol 24-hydroxylase gene in mice reveals a brain-specific mechanism of cholesterol turnover. *J Biol Chem* 2003;278:22980–22988.
- Erickson SK, Lear SR, Deane S, Dubrac S, Huling SL, Nguyen L, Bollineni JS, Shefer S, Hyogo H, Cohen DE, Shneider B, Sehayek E, Ananthanarayanan M, Balasubramanian N, Suchy FJ, Batta AK, Salen G. Hypercholesterolemia and changes in lipid and bile acid metabolism in male and female cyp7A1-deficient mice. *J Lipid Res* 2003;44:1001–1009.
- McMillin M, Frampton G, Grant S, Khan S, Diocares J, Petrescu A, Wyatt A, Kain J, Jefferson B, DeMorrow S. Bile acid-mediated sphingosine-1-phosphate receptor 2 signaling promotes neuroinflammation during hepatic encephalopathy in mice. *Front Cell Neurosci* 2017;11:191.
- McMillin M, Galindo C, Pae HY, Frampton G, Di Patre PL, Quinn M, Whittington E, DeMorrow S. Gli1 activation and protection against hepatic encephalopathy is suppressed by circulating transforming growth factor beta1 in mice. *J Hepatol* 2014;61:1260–1266.
- McMillin M, Grant S, Frampton G, Andry S, Brown A, DeMorrow S. Fractalkine suppression during hepatic encephalopathy promotes neuroinflammation in mice. *J Neuroinflammation* 2016;13:198.
- Pol A, Luetterforst R, Lindsay M, Heino S, Ikonen E, Parton RG. A caveolin dominant negative mutant associates with lipid bodies and induces intracellular cholesterol imbalance. *J Cell Biol* 2001;152:1057–1070.
- Vanier MT, Latour P. Laboratory diagnosis of Niemann–Pick disease type C: the filipin staining test. *Methods Cell Biol* 2015;126:357–375.
- Frampton G, Invernizzi P, Bernuzzi F, Pae HY, Quinn M, Horvat D, Galindo C, Huang L, McMillin M, Cooper B, Rimassa L, DeMorrow S. Interleukin-6-driven progranulin expression increases cholangiocarcinoma growth by an Akt-dependent mechanism. *Gut* 2012;61:268–277.
- DeMorrow S, Francis H, Gaudio E, Venter J, Franchitto A, Kopriva S, Onori P, Mancinelli R, Frampton G, Coufal M, Mitchell B, Vaculin B, Alpini G. The endocannabinoid anandamide inhibits cholangiocarcinoma growth via activation of the noncanonical Wnt signaling pathway. *Am J Physiol Gastrointest Liver Physiol* 2008;295:G1150–G1158.
- Livak KJ, Schmittgen TD. Analysis of relative gene expression data using real-time quantitative PCR and the 2⁻(delta delta C(T)) method. *Methods* 2001;25:402–408.
- Song P, Rockwell CE, Cui JY, Klaassen CD. Individual bile acids have differential effects on bile acid signaling in mice. *Toxicol Appl Pharmacol* 2015;283:57–64.
- Powell E, Anch AM, Dyche J, Bloom C, Richtert RR. The splay angle: a new measure for assessing neuromuscular dysfunction in rats. *Physiol Behav* 1999;67:819–821.
- Davidson CD, Ali NF, Micsenyi MC, Stephney G, Renault S, Dobrenis K, Ory DS, Vanier MT, Walkley SU. Chronic cyclodextrin treatment of murine Niemann–Pick C disease ameliorates neuronal cholesterol and glycosphingolipid storage and disease progression. *PLoS One* 2009;4:e6951.
- Butterworth RF, Norenberg MD, Felipo V, Ferenci P, Albrecht J, Blei AT. Members of the ISHEN Commission on Experimental Models of HE. Experimental models of hepatic encephalopathy: ISHEN guidelines. *Liver Int* 2009;29:783–788.
- Hori T, Chen F, Baine AM, Gardner LB, Nguyen JH. Fulminant liver failure model with hepatic encephalopathy in the mouse. *Ann Gastroenterol* 2011;24:294–306.
- Jayakumar AR, Ruiz-Cordero R, Tong XY, Norenberg MD. Brain edema in acute liver failure: role of neurosteroids. *Arch Biochem Biophys* 2013;536:171–175.
- McMillin MA, Frampton GA, Seiwel AP, Patel NS, Jacobs AN, DeMorrow S. TGFbeta1 exacerbates blood-brain barrier permeability in a mouse model of hepatic encephalopathy via upregulation of MMP9 and down-regulation of claudin-5. *Lab Invest* 2015;95:903–913.

22. Nguyen JH, Yamamoto S, Steers J, Sevelev D, Lin W, Shimojima N, Castanedes-Casey M, Genco P, Golde T, Richelson E, Dickson D, McKinney M, Eckman CB. Matrix metalloproteinase-9 contributes to brain extravasation and edema in fulminant hepatic failure mice. *J Hepatol* 2006;44:1105–1114.
23. Chastre A, Belanger M, Nguyen BN, Butterworth RF. Lipopolysaccharide precipitates hepatic encephalopathy and increases blood-brain barrier permeability in mice with acute liver failure. *Liver Int* 2014;34:353–361.
24. Chastre A, Jiang W, Desjardins P, Butterworth RF. Ammonia and proinflammatory cytokines modify expression of genes coding for astrocytic proteins implicated in brain edema in acute liver failure. *Metab Brain Dis* 2010;25:17–21.
25. Felipo V, Urios A, Montesinos E, Molina I, Garcia-Torres ML, Civera M, Olmo JA, Ortega J, Martinez-Valls J, Serra MA, Cassinello N, Wassel A, Jorda E, Montoliu C. Contribution of hyperammonemia and inflammatory factors to cognitive impairment in minimal hepatic encephalopathy. *Metab Brain Dis* 2012;27:51–58.
26. Acharya C, Bajaj JS. Gut microbiota and complications of liver disease. *Gastroenterol Clin North Am* 2017;46:155–169.
27. Horvatits T, Drolz A, Roedl K, Rutter K, Ferlitsch A, Fauler G, Trauner M, Fuhrmann V. Serum bile acids as marker for acute decompensation and acute-on-chronic liver failure in patients with non-cholestatic cirrhosis. *Liver Int* 2017;37:224–231.
28. Kawamata Y, Fujii R, Hosoya M, Harada M, Yoshida H, Miwa M, Fukusumi S, Habata Y, Itoh T, Shintani Y, Hinuma S, Fujisawa Y, Fujino MA. G protein-coupled receptor responsive to bile acids. *J Biol Chem* 2003;278:9435–9440.
29. McMillin M, DeMorrow S. Effects of bile acids on neurological function and disease. *FASEB J* 2016;30:3658–3668.
30. Nardone R, De Blasi P, Holler Y, Brigo F, Golaszewski S, Frey VN, Orioli A, Trinkka E. Intracortical inhibitory and excitatory circuits in subjects with minimal hepatic encephalopathy: a TMS study. *Metab Brain Dis* 2016;31:1065–1070.
31. Chen QF, Chen HJ, Liu J, Sun T, Shen QT. Machine learning classification of cirrhotic patients with and without minimal hepatic encephalopathy based on regional homogeneity of intrinsic brain activity. *PLoS One* 2016;11:e0151263.
32. Milagre I, Nunes MJ, Gama MJ, Silva RF, Pascussi JM, Lechner MC, Rodrigues E. Transcriptional regulation of the human CYP46A1 brain-specific expression by Sp transcription factors. *J Neurochem* 2008;106:835–849.
33. Tu AY, Albers JJ. Functional analysis of the transcriptional activity of the mouse phospholipid transfer protein gene. *Biochem Biophys Res Commun* 2001;287:921–926.
34. Vance JE. Dysregulation of cholesterol balance in the brain: contribution to neurodegenerative diseases. *Dis Model Mech* 2012;5:746–755.
35. DeBarber AE, Eroglu Y, Merkens LS, Pappu AS, Steiner RD. Smith-Lemli-Opitz syndrome. *Expert Rev Mol Med* 2011;13:e24.
36. Leoni V, Caccia C. The impairment of cholesterol metabolism in Huntington disease. *Biochim Biophys Acta* 2015;1851:1095–1105.
37. Klein AD, Alvarez A, Zanolungo S. The unique case of the Niemann-Pick type C cholesterol storage disorder. *Pediatr Endocrinol Rev* 2014;12(Suppl 1):166–175.
38. Butterworth RF. Neurosteroids in hepatic encephalopathy: novel insights and new therapeutic opportunities. *J Steroid Biochem Mol Biol* 2016;160:94–97.
39. Pucadyil TJ, Chattopadhyay A. Role of cholesterol in the function and organization of G-protein coupled receptors. *Prog Lipid Res* 2006;45:295–333.
40. Smith AJ, Sugita S, Charlton MP. Cholesterol-dependent kinase activity regulates transmitter release from cerebellar synapses. *J Neurosci* 2010;30:6116–6121.
41. Metais C, Hughes B, Herron CE. Simvastatin increases excitability in the hippocampus via a PI3 kinase-dependent mechanism. *Neuroscience* 2015;291:279–288.
42. Cuddy LK, Winick-Ng W, Rylett RJ. Regulation of the high-affinity choline transporter activity and trafficking by its association with cholesterol-rich lipid rafts. *J Neurochem* 2014;128:725–740.
43. Megias-Vericat JE, Garcia-Robles A, Company-Albir MJ, Fernandez-Megia MJ, Perez-Mirallas FC, Lopez-Briz E, Casanova B, Poveda JL. Early experience with compassionate use of 2-hydroxypropyl-beta-cyclodextrin for Niemann-Pick type C disease: review of initial published cases. *Neurol Sci* 2017;38:727–743.
44. Ory DS, Ottinger EA, Farhat NY, King KA, Jiang X, Weissfeld L, Berry-Kravis E, Davidson CD, Bianconi S, Keener LA, Rao R, Soldatos A, Sidhu R, Walters KA, Xu X, Thurm A, Solomon B, Pavan WJ, Machielse BN, Kao M, Silber SA, McKew JC, Brewer CC, Vite CH, Walkley SU, Austin CP, Porter FD. Intrathecal 2-hydroxypropyl-beta-cyclodextrin decreases neurological disease progression in Niemann-Pick disease, type C1: a non-randomised, open-label, phase 1-2 trial. *Lancet* 2017;390:1758–1768.
45. Vance JE, Peake KB. Function of the Niemann-Pick type C proteins and their bypass by cyclodextrin. *Curr Opin Lipidol* 2011;22:204–209.

Received February 1, 2018. Accepted February 26, 2018.

Correspondence

Address correspondence to: Sharon DeMorrow, PhD, Department of Medical Physiology, Texas A&M Health Science Center, Central Texas Veterans Health Care System, Building 205, 1901 South 1st Street, Temple, Texas 76704. e-mail: demorrow@medicine.tamhsc.edu; fax: (254) 743-0378.

Acknowledgments

The authors would like to acknowledge Amy Wyatt for her technical expertise. This material is the result of work supported with resources and the use of facilities at the Central Texas Veterans Health Care System (Temple, TX).

Author contributions

Matthew McMillin and Sharon DeMorrow were responsible for the study concept and design; Matthew McMillin, Stephanie Grant, Gabriel Frampton, Anca D. Petrescu, Jessica Kain, Elaina Williams, Rebecca Haines, Lauren Canady, and Sharon DeMorrow acquired data; Matthew McMillin, Stephanie Grant, Gabriel Frampton, Anca D. Petrescu, Jessica Kain, Elaina Williams, Rebecca Haines, Lauren Canady, and Sharon DeMorrow analyzed and interpreted data; Matthew McMillin and Sharon DeMorrow drafted the manuscript; Matthew McMillin, Stephanie Grant, Gabriel Frampton, Anca D.

Petrescu, Jessica Kain, Elaina Williams, Rebecca Haines, Lauren Canady, and Sharon DeMorrow critically revised the manuscript for important intellectual content; Matthew McMillin, Stephanie Grant, Gabriel Frampton, Anca D. Petrescu, Jessica Kain, Elaina Williams, Rebecca Haines, Lauren Canady, and Sharon DeMorrow performed the statistical analysis; and Matthew McMillin and Sharon DeMorrow obtained funding.

Conflicts of interest

The authors disclose no conflicts.

Funding

This study was funded by a National Institutes of Health R01 award (DK082435) and a VA Merit award (BX002638) from the US Department of Veterans Affairs Biomedical Laboratory Research and Development Service (S.D.), and by a VA Career Development award (BX003486) from the US Department of Veterans Affairs Biomedical Laboratory Research and Development Service (M.M.). The content is the responsibility of the author(s) alone and does not necessarily reflect the views or policies of the Department of Veterans Affairs or the United States Government.